Label-free optical imaging of mitochondria in live cells

David Lasne[1], Gerhard. A. Blab[1], Francesca De Giorgi[2], François Ichas[2], Brahim Lounis[1] and Laurent Cognet[1*]

[1]Centre de Physique Moléculaire Optique et Hertzienne, Université Bordeaux 1, and CNRS, Talence, F-33405 France
[2]INSERM E347, Institut Bergonié, 229 cours de l'Argonne, 33000 Bordeaux, France
**Corresponding author: lcognet@u-bordeaux1.fr*
http://www.cpmoh.cnrs.fr/nanophotonics

Abstract: The far-field optical imaging of mitochondria of live cells without the use of any label is demonstrated. It uses a highly sensitive photothermal method and has a resolution comparable to confocal fluorescence setups. The morphological states of mitochondria were followed under different physiological treatments, and the role of cytochrome c was ruled out as the main origin of the photothermal signals. This label free optical method provides a high contrast imaging of live mitochondria and should find many applications in biosciences.

OCIS codes: (170.3880) Medical and Biomedical Imaging; (170.4580) Optical diagnostic for Medicine; (190.4870) Optically induced thermo-optical effects; (180.3170) Interference Microscopy.

References and links

1. D. J. Stephens and V. J. Allan, "Light microscopy techniques for live cell imaging," Science **300**, 82-86 (2003).
2. J. R. Gledhill and J. E. Walker, "Inhibition in F1-ATPase from bovine heart mitochondria," Biochem. J. **386**, 591 (2005).
3. L. Scorrano, V. Petronilli, R. Colonna, F. Di Lisa, and P. Bernardi, "Chloromethyltetramethylrosamine (Mitotracker Orange) induces the mitochondrial permeability transition and inhibits respiratory complex I. Implications for the mechanism of cytochrome c release," J Biol. Chem **274**, 24657-24663 (1999).
4. J. F. Buckman, H. Hernandez, G. J. Kress, T. V. Votyakova, S. Pal, and I. J. Reynolds, "MitoTracker labeling in primary neuronal and astrocytic cultures: influence of mitochondrial membrane potential and oxidants," J. Neurosci. Method. **104**, 165 (2001).
5. S. DiMauro, "Mitochondrial myopathies," Curr Opin Rheumatol **18**, 636-641 (2006).
6. P. L. Gourley, J. K. Hendricks, A. E. McDonald, R. G. Copeland, K. E. Barrett, C. R. Gourley, K. K. Singh, and R. K. Naviaux, "Mitochondrial correlation microscopy and nanolaser spectroscopy - new tools for biophotonic detection of cancer in single cells," Technol. Cancer Res Treat **4**, 585-592 (2005).
7. S. Berciaud, L. Cognet, G. A. Blab, and B. Lounis, "Photothermal Heterodyne Imaging of Individual Nonfluorescent Nanoclusters and Nanocrystals," Phys Rev Lett **93**, 257402 (2004).
8. M. A. Van Dijk, A. L. Tchebotareva, M. Orrit, M. Lippitz, S. Berciaud, D. Lasne, L. Cognet, and B. Lounis, "Absorption and scattering microscopy of single metal nanoparticles," Phys. Chem. Chem. Phys. **8**, 3486 (2006).
9. S. Berciaud, D. Lasne, G. A. Blab, L. Cognet, and B. Lounis, "Photothermal Heterodyne Imaging of Individual Metallic Nanoparticles: Theory versus Experiments," Phys. Rev. B **73**, 045424 (2006).
10. G. A. Blab, L. Cognet, S. Berciaud, I. Alexandre, D. Husar, J. Remacle, and B. Lounis, "Optical readout of gold nanoparticle-based DNA microarrays without silver enhancement," Biophys. J. **90** (2006).
11. E. Tamaki, K. Sato, M. Tokeshi, K. Sato, M. Aihara, and T. Kitamori, "Single-cell analysis by a scanning thermal lens microscope with a microchip: direct monitoring of cytochrome c distribution during apoptosis process," Anal Chem **74**, 1560-1564 (2002).
12. V. P. Zharov, V. Galitovskiy, C. S. Lyle, and T. C. Chambers, "Superhigh-sensitivity photothermal monitoring of individual cell response to antitumor drug," J Biomed Opt **11**, 064034 (2006).
13. L. A. Ligon, and O. Steward, "Movement of mitochondria in the axons and dendrites of cultured hippocampal neurons," J. Comp. Neurol. **427**, 340-350 (2000).
14. C. Hoppel, and C. Cooper, "The action of digitonin on rat liver mitochondria. The effects on enzyme content," Biochem. J. **107**, 367-375 (1968).

#85286 - $15.00 USD Received 17 Jul 2007; revised 7 Sep 2007; accepted 11 Sep 2007; published 12 Oct 2007

15. A. E. Vercesi, C. F. Bernardes, M. E. Hoffmann, F. R. Gadelha, and R. Docampo, "Digitonin permeabilization does not affect mitochondrial function and allows the determination of the mitochondrial membrane potential of Trypanosoma cruzi in situ," J Biol Chem **266**, 14431-14434 (1991).
16. R. Rizzuto, M. Brini, P. Pizzo, M. Murgia, and T. Pozzan, "Chimeric green fluorescent protein as a tool for visualizing subcellular organelles in living cells," Curr. Biol. **5**, 635 (1995).
17. R. M. Kluck, E. Bossy-Wetzel, D. R. Green, and D. D. Newmeyer, "The release of cytochrome c from mitochondria: a primary site for Bcl-2 regulation of apoptosis," Science **275**, 1132-1136 (1997).
18. J. Yang, X. Liu, K. Bhalla, C. N. Kim, A. M. Ibrado, J. Cai, T. I. Peng, D. P. Jones, and X. Wang, "Prevention of apoptosis by Bcl-2: release of cytochrome c from mitochondria blocked," Science **275**, 1129-1132 (1997).
19. J. C. Goldstein, N. J. Waterhouse, P. Juin, G. I. Evan, and D. R. Green, "The coordinate release of cytochrome c during apoptosis is rapid, complete and kinetically invariant," Nat Cell Biol **2**, 156-162 (2000).
20. D. DiDonato, and D. L. Brasaemle, "Fixation Methods for the Study of Lipid Droplets by Immunofluorescence Microscopy," J. Histochem. Cytochem. **51**, 773-780 (2003).
21. P. G. Heytler, "Uncoupling of Oxidative Phosphorylation by Carbonyl Cyanide Phenylhydrazones. I. Some Characteristics of m-CI-CCP Action on Mitochondria and Chloroplasts," Biochemistry **2**, 357-361 (1963).
22. R. A. Goldsby, and P. G. Heytler, "Uncoupling Of Oxidative Phosphorylation By Carbonyl Cyanide Phenylhydrazones. Ii. Effects Of Carbonyl Cyanide M-Chlorophenylhydrazone On Mitochondrial Respiration," Biochemistry **2**, 1142-1147 (1963).
23. B. Z. Cavari, and Y. Avi-Dor, "Effect of carbonyl cyanide m-chlorophenylhydrazone on respiration and respiration-dependent phosphorylation in Escherichia coli," Biochem. J. **103**, 601-608 (1967).
24. W. Gao, Y. Pu, K. Q. Luo, and D. C. Chang, "Temporal relationship between cytochrome c release and mitochondrial swelling during UV-induced apoptosis in living HeLa cells," J. Cell Sci. **114**, 2855-2862 (2001).
25. I. Agalidis, S. Othman, A. Boussac, F. Reiss-Husson, and A. Desbois, "Purification, redox and spectroscopic properties of the tetraheme cytochrome c isolated from Rubrivivax gelatinosus," Eur. J. Biochem. **261**, 325 (1999).
26. T. J. Sick, and M. A. Perez-Pinzon, "Optical methods for probing mitochondrial function in brain slices," Methods **18**, 104-108 (1999).
27. A. J. Borgdorff, and D. Choquet, "Regulation of AMPA receptor lateral movements," Nature **417**, 649-653. (2002).
28. R. Bertrand, E. Solary, P. O'Connor, K. W. Kohn, and Y. Pommier, "Induction of a common pathway of apoptosis by staurosporine," Exp. Cell Res. **211**, 314-321 (1994).

1. Introduction

Precise imaging of tissues or cellular structure is extremely useful for fundamental research in biology as well as for medical applications. Optical methods are especially well suited for this purpose as they are non-invasive. Most biological exhibit a rather low optical contrast, and even if sensitive microscopy techniques such as Phase Contrast or Differential Interference Contrast can reveal some intracellular structures of live cells [1], most organelles remain hidden with white light microscopes. To gain specificity and contrast, fluorescent molecules are commonly used to label particular target components and report their localization. Such labels which include organic fluorophores or autofluorescent proteins may however interfere with cellular activity. For instance, Rhodamine6G or MitoTracker Orange can interfere with mitochondrial respiration [2] [3]. In addition, the label-target complex may have different behavior from the native target and the labeling specificity and efficiency can vary according to experimental conditions [4].

In this work, we report the far-field optical imaging of mitochondria of live cells without the use of any label. High quality imaging of mitochondria is of great interest for medical applications. In particular, the shape, spatial distribution, and aggregation of mitochondria can be markers for identifying some myopathies[5] or cancer cells, as previously demonstrated with fluorescence labeling techniques [6].

Here we used an ultra-sensitive photothermal method developed recently for the detection individual absorbing nano-objects[7, 8]. This method referred as Light Induced Scattering Around a NanoAbsorber (LISNA) was used to ultimately detect gold nanoparticles as small as 1.4 nm in diameter[7, 9] and is applicable in different fields of science such as for the improvement of DNA chips[10]. Owing to its unsurpassed sensitivity in detecting absorbing nano-objects, LISNA was the natural candidate to perform high resolutions far-field optical

#85286 - $15.00 USD Received 17 Jul 2007; revised 7 Sep 2007; accepted 11 Sep 2007; published 12 Oct 2007

images of mitochondria in live cells, a well-known light absorbing cellular organelle. This assumption was further encouraged by the earlier detection of extracts of mitochondria, by a thermal lens microscope [11]. A photothermal assay that is sensitive to mitochondrial morphology [12] has also been proposed more recently with potential for identifying cancer cells but still suffer from poor resolution capabilities. In both of these studies, cytochrome c, a heme highly present in mitochondria was assumed to be at the origin of the signals.
In our work, the much higher sensitivity over previous methods and confocal-like resolution allow a systematic study of mitochondria morphology as a function of cellular state. Our results rule out the main contribution of cytochrome c in the mitochondrial photothermal signals, which is in contrast to previous assumptions.

2. Optical setup

The experimental setup combines LISNA, confocal fluorescence and white light microscopy capabilities for live cell imaging on the same instrument (Fig. 1).

2.1 Principle of LISNA

The precise description of LISNA has been described elsewhere in the case of metal spherical nanoparticles [7, 9]. We will here briefly remind its principle for the general case of a nanometer sized light absorber that releases the majority of its absorbed energy into heat when exposed to light. The corresponding increase of temperature around the absorber gives rise to a local variation of the refraction index. LISNA uses a combination of a focused time-modulated heating beam and a focused non-resonant probe beam. The heating induces a time-modulated variation of the refraction index around the absorbing object. The interaction of the probe beam with this index profile produces a scattered field with sidebands at the modulation frequency. The scattered field is then detected in the forward direction through its beatnote with the transmitted probe field which plays the role of a local oscillator akin a heterodyne technique. Raster-scan of a sample containing nano-absorbers produces 2D LISNA images of the sample (see Fig. 1).

When a characteristic dimension of a light absorber is comparable to or larger than the heating beam, the signal originates from the total spatial distribution of the modulated refraction index encountered by the probe beam which can also include a non-negligible contribution from the object itself.

2.2 LISNA setup

A non-resonant probe beam (HeNe, 632.8 nm) and an absorbed exciting beam (532 nm, frequency doubled Nd:YAG laser or Argon laser) are overlaid and focused on the sample by means of a high NA microscope objective (100×, NA=1.4). The intensity of the exciting beam is modulated at a frequency Ω (typically $\Omega/2\pi$ = 700 kHz) by an acousto-optic modulator. A second microscope objective (80×, NA=0.8) collects the interfering probe-transmitted and forward-scattered fields. The intensity of the exciting beam sent on the samples was 200 kW/cm^2. The forward interfering fields are collected on a fast photodiode and fed into a lock-in amplifier in order to extract the beat signal at Ω. Integration times of 5 ms per pixel are used. 2D images are performed by moving the sample in the plane transverse to the optical axis of the fixed laser spots by means of a 3D piezo-scanner.

2.3 Confocal fluorescence setup

The same microscope allows performing confocal fluorescence imaging. The He-Ne laser (resp. an Argon laser line at 488 nm) is used to excite Mitotracker Deep Red (resp. Alexa 488) and focused on the sample (100 W/cm^2). The emitted light is collected backwards, filtered by an emission filter (HQ 700/100, resp. HQ 525/50) and focused on an avalanche photodiode. Integration times of 1 ms are used. Images are performed similarly to LISNA images, by moving the sample over the fixed laser spot by means of the piezo-scanner.

#85286 - $15.00 USD Received 17 Jul 2007; revised 7 Sep 2007; accepted 11 Sep 2007; published 12 Oct 2007

2.4 Resolution

LISNA imaging was designed to detect single absorbing nano-objects. The refractive index profile due to the local heating of the nano-absorber extends over a few tenths of nanometers around it, which remains far smaller than optical wavelengths. The interaction of the probe beam with that profile was then described using a light scattering theory by a fluctuating dielectric medium [9]. It follows that the point spread function is given by the product of the probe and heating beam profiles [9], which is 310 ± 4 nm (FWHM) with our geometry.
Mitochondria however are larger objects than a single nano-absorber and contain several absorbing species. In that case, a variety of absorbing molecules at the focal point of the exciting beam might contribute to the local heating over a few hundreds of nanometers.

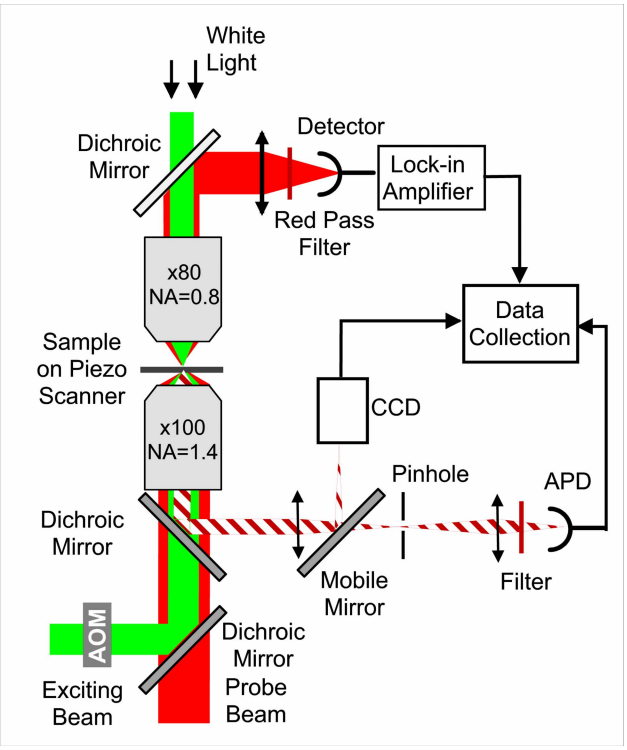

Fig. 1. Experimental setup combining multi-imaging capabilities. LISNA uses the exciting beam which intensity is modulated with an acousto-optic modulator (AOM), the probe beam, the upper detector and the lock-in amplifier. For confocal fluorescence imaging, either the excitation or probe beam are used depending on the fluorophore to be excited and the fluorescence is filtered and detected by the avalanche photodiode (APD). For creating 2D images the sample is raster scanned by means of the piezo-scanner both for LISNA and confocal fluorescence imaging. White light is used to perform large field images of the sample that are recorded the CCD camera.

3. Detection of mitochondria in live cells

LISNA imaging of live COS-7 cells revealed intrinsic signals (without any labeling) from well defined organelles which shapes and characteristic localizations (around the nucleus) remind that of mitochondria (Fig. 2). This assumption is confirmed by comparing LISNA and confocal fluorescence images of specifically labeled mitochondria successively performed on the same cells (Mitotracker Deep Red). A clear colocalization of both signals is observed, as

#85286 - $15.00 USD Received 17 Jul 2007; revised 7 Sep 2007; accepted 11 Sep 2007; published 12 Oct 2007

shown in Fig. 2. This experiment was also performed on hippocampal neurons, leading to the same conclusion (Fig. 3).

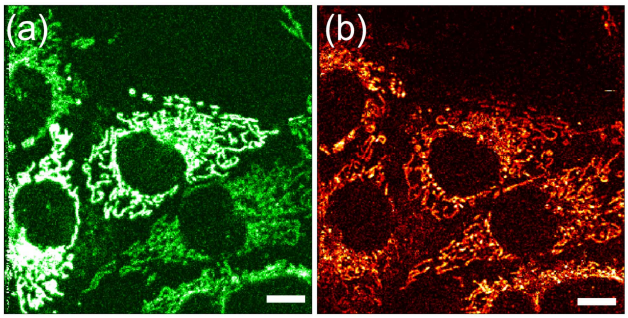

Fig. 2. (a). Fluorescence (Mitotracker Deep Red) and (b) LISNA images of COS-7 cells. The scale bar represents 10 µm.

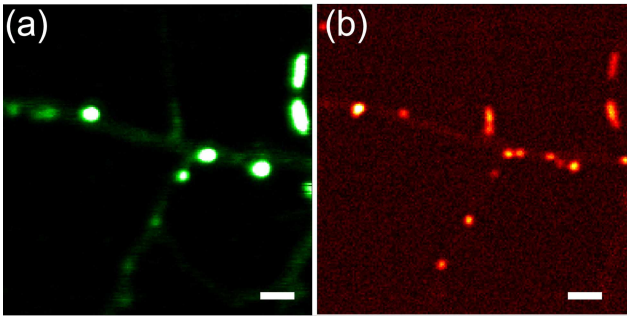

Fig.3. (a). Fluorescence (Mitotracker Deep Red) and (b) LISNA images of hippocampal neurons. The scale bar represents 2 µm.

Some subtle localization differences can be identified on Figs. 2 and 3 between LISNA and fluorescence images. These can be attributed to slight mitochondrial movements and shape changes in the live cells as previously observed [13]. At the higher magnification used in Fig. 3 these movements are more visible. Moreover, LISNA images show better resolved structures, due to a greater spatial resolution achieved by LISNA than by our fluorescence setup. In COS-7 cells or cultured neurons, the mitochondria are mostly distributed in a plane such that the 2D images presented here give the complete structural information without the need of the sectioning capabilities offered by LISNA that are comparable to confocal imaging (not shown). Finally, one can notice the fluorescence labeling is rather heterogeneous and some cells appear brighter than others. This is due to variations of the labeling specificity and efficiency of Mitotracker that vary from cell to cell and with experimental conditions [4]. This extrinsic pitfall does not apply with LISNA images.

4. Origin of the signals

Previous studies have assumed that mitochondrial photothermal contrast originates from an inter-membrane mitochondrial protein, cytochrome c, which is known to be quite a strong absorber for visible wavelength [11] [12]. In the following, the greater sensitivity and resolution of LISNA over previous methods will be used to challenge this assumption and seek the origin of the mitochondrial contrast. For this purpose, the morphological, structural and physiological states of mitochondria will be changed and analyzed with LISNA images.

#85286 - $15.00 USD Received 17 Jul 2007; revised 7 Sep 2007; accepted 11 Sep 2007; published 12 Oct 2007

4.1 Influence of mitochondrial external membrane permeabilization induced by digitonin

The effect of mitochondrial membrane permeabilization is first presented. Live COS-7 cells were imaged before and after addition of 100µM digitonin which solubilizes lipids and pierces cell membranes. It also permeabilizes the mitochondrial external membrane [14] [15]. We ensured that the inner membrane was not affected during this treatment by testing it on cells transfected with mtGFP (a GFP targeted to the mitochondrial matrix by fusion with the presequence of the subunit VIII of cytochrome c oxidase [16]) : this matrix protein remains localized in mitochondria after treatment with 100µM digitonin (data not shown).

After several minutes (typically 5 min, which basically corresponds to the time for taking one image), a clear decrease and almost total extinction of the signal was found, as shown in Fig. 4 indicating that the signal must originate from an inter-membrane component or linked to the external membrane of the mitochondria. In this context, cytochrome c is a good candidate.

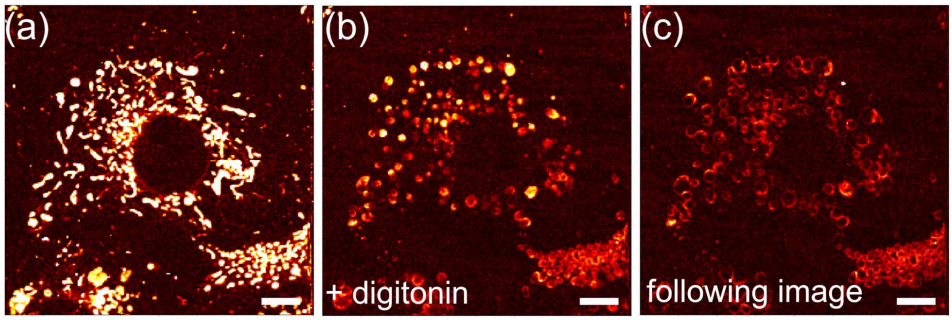

Fig. 4. LISNA images of COS-7 cells portions before (a) and after (b,c) 100 mM digitonin loading (The scale bar represents 10 µm).

4.2 Cytochrome c release experiments

Interestingly, cytochrome c is released into cytosol during apoptosis[17, 18]. If LISNA contrast originates from cytochrome c, the signal should vanish during apoptosis. To test this hypothesis, we thus treated HeLa cells with staurosporin (STS) to induce apoptosis in presence of zVAD-fmk to inhibit caspase activity and thus preserve cell morphology[19]. After 6-8 hours, cells were fixed and cytochrome c was detected by indirect immunofluorescence, with secondary antibodies labeled with Alexa 488 (see Methods).

We then performed both fluorescence and LISNA imaging on the same setup. While most cells (corresponding with cells which did not react to STS) exhibit a well structured fluorescence signal from labeled cytochrome c in mitochondria, some (10-20 %) cells exhibit a very diffuse signal as cytochrome c was released into cytosol (Fig. 5). The LISNA signal however remains really structured even on apoptotic cells. We thus concluded that LISNA signal cannot be primarily attributed to cytochrome c. Moreover, one can reasonably think that it is not due to any of the inter-membrane proteins that are released during apoptosis.

#85286 - $15.00 USD Received 17 Jul 2007; revised 7 Sep 2007; accepted 11 Sep 2007; published 12 Oct 2007

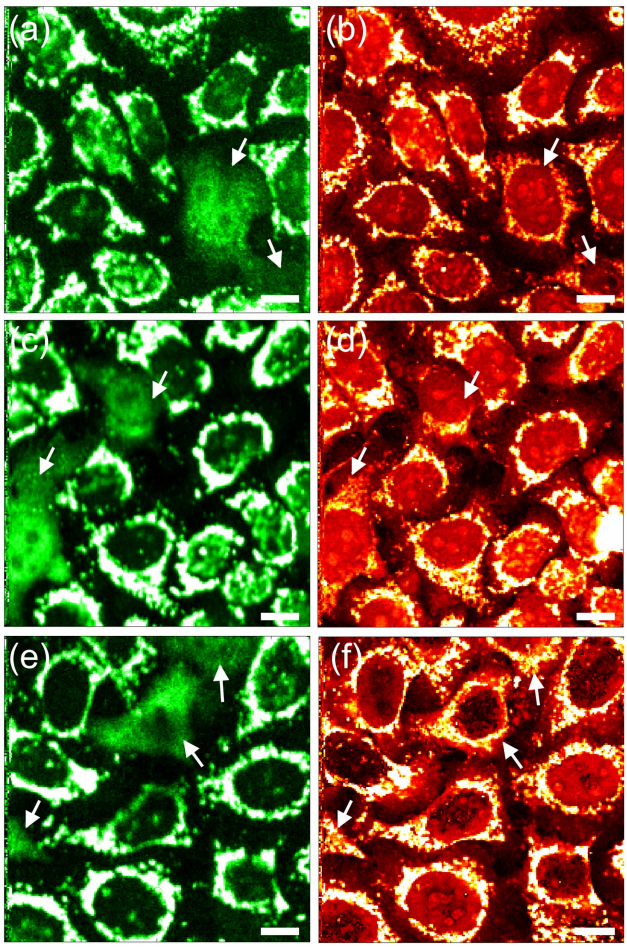

Fig. 5. Images of HeLa cells after apoptosis induction using staurosporin (The scale bar represents 10 µm). (a,c,e) Fluorescence images. Cytochrome c is fluorescently labeled and localized in mitochondria for most cells. But some cells (arrows) show very diffuse signal as cytochrome c is released into the cytosol during apoptosis. However, the LISNA signal (b,d,f) is very structured, even in those cells.

4.3 Mitochondrial membrane phospholipids

We also investigated the possible role of some mitochondrial membrane phospholipids in the detected signal. For this purpose, COS-7 cells were fixed using pre-cooled (-18°C) methanol. This fixation protocol is known to remove most cellular phospholipids [20]. Cells were then imaged with LISNA. Mitochondria were still visible with comparable signal to noise ratio (data not shown). Note that cells fixation using paraformaldehyde does not influence LISNA mitochondrial signals (data not shown).

4.4 Influence of mitochondrial membrane depolarization induced by carbonyl cyanide m-chlorophenylhydrazone (CCCP)

We then investigated the possible effect of mitochondrial membrane depolarization on the LISNA detection of mitochondria. For this purpose, live COS-7 cells were imaged before and after addition of 1µM carbonyl cyanide m-chlorophenylhydrazone (CCCP), a highly toxic ionophore and decoupler of the respiratory chain [21-23].

#85286 - $15.00 USD Received 17 Jul 2007; revised 7 Sep 2007; accepted 11 Sep 2007; published 12 Oct 2007

No change in the signal intensity was found, but a conformational change of the mitochondria was clearly visible, from elongated to circle structures (see Fig. 6). This constitutes a known effect of CCCP [24] but imaged here without staining. This indicates that the LISNA signal is membrane potential independent.

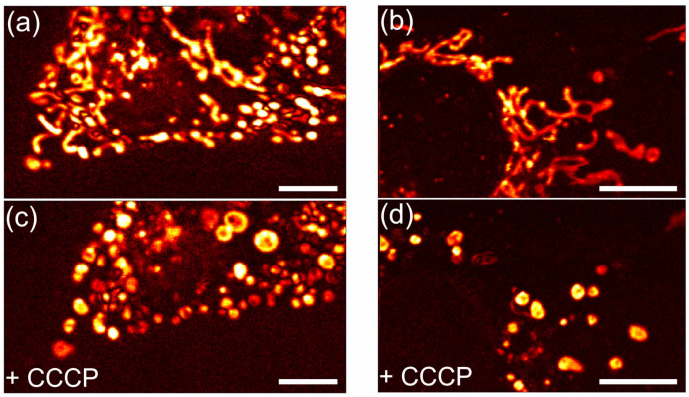

Fig. 6. LISNA images of COS-7 cells portions before (a,b) and after (c,d) 1µM CCCP loading (The scale bar represents 10 µm).

4.5 Influence of excitation wavelength

Many mitochondrial proteins, such as cytochromes, have been isolated and their optical response is well characterized [25]. Most of those components have strong absorption bands in the visible range that vary depending on experimental conditions [26]. We thus tested the influence of excitation wavelength on the detected signal. We replaced the frequency doubled Nd:YAG laser (532 nm) by an Argon laser (458 nm, 488 nm or 514 nm lines) and compared images of live COS-7 cells obtained at different wavelength (at identical exciting intensity). A 2 fold decrease of the signal was observed between 458 nm and higher wavelength. This was further corroborated with absorption spectra of a suspension of mitochondria measured in bulk with spectrophotometer where no clear effect of the wavelength was visible, except a smooth decrease from short (400nm) to long (1000nm) wavelengths (data not shown).

5. Conclusion

In this work, the unequalled sensitivity and resolution of LISNA imaging over previous methods allow a systematic study of intrinsic mitochondria morphology as a function of cellular state. In contrast to previous studies that have assigned mitochondrial photothermal contrast to cytochrome c, our work clearly indicates that it has another origin. Our date indicate that it might be due to an ensemble of proteins that are present near the mitochondrial membrane, in a non-specific manner. Further studies will be needed to fully understand the origin of the signal. We foresee due to its high contrast, insensitivity to any background (autofluorescence or scattering), and high resolution, this method has the potential of an efficient diagnostic tool, and should find numerous application in biosciences.

6. Biological Methods

6.1 Cell culture, MitoTracker staining

COS-7 and HeLa cells were cultured in DMEM medium supplemented with streptomycin (100 µg/ml), penicillin (100 U/ml), and 10% bovine serum in a humidified atmosphere (95%) at 5% CO_2 and 37^{o}C. Cells were used for 12-14 passages and were transferred every 4 days.

#85286 - $15.00 USD Received 17 Jul 2007; revised 7 Sep 2007; accepted 11 Sep 2007; published 12 Oct 2007

The coverslips were mounted in a custom open chamber with culture medium supplemented with 20 mM Hepes, pH 7.4. All data were taken at room temperature.
For fluorescence imaging, the coverslips were incubated 1 min at room temperature with 3 µM MitoTracker Deep Red. After three rinses in culture medium, the coverslips were mounted in the chamber.

6.2 Neuron culture, MitoTracker staining

Hippocampal neurons from 18 days old rat embryos were cultured on glass coverslips as previously [27]. The coverslips were mounted in a custom open chamber with culture medium supplemented with 20 mM Hepes, pH 7.4. All data were taken at room temperature.
For fluorescence imaging, the coverslips were incubated 1 min at room temperature with 3 µM MitoTracker Deep Red. After three rinses in culture medium, the coverslips were mounted in the chamber.

6.3 CCCP experiments

To probe the possible effect of mitochondrial membrane depolarization on the signal, samples were treated with Carbonyl cyanide m-chlorophenylhydrazone (CCCP). After several images under normal condition (culture medium), we changed half of the medium and replaced it with medium loaded with CCCP so that the final concentration was 1µM. Images were taken just after CCCP loading.

6.4 Digitonin experiments

To probe the possible effect of mitochondrial membrane permeabilization on the signal, samples were treated with digitonin. After several images under normal condition (culture medium), we removed the medium and replaced it with intracellular medium loaded with digitonin at 100 µM. Images were taken just after digitonin loading.

6.5 Cell fixation

Paraformaldehyde Fixation: medium was removed from the cells, which were then washed twice with PBS. Cells were incubated with 3% paraformaldehyde in PBS for 15 minutes at room temperature and then washed three times with PBS and mounted on glass slides using mowiol.
Methanol/Acetone Fixation: methanol was stored at -18°C before use. The culture medium was removed and the cells on coverslips were washed twice with PBS. The cells were incubated with cold methanol in a prechilled glass tray kept on ice for 10 min, and then were washed three times with PBS. For fixation with acetone, we used the same protocol.

6.6 Cytochrome c release experiments

We treated HeLa cells with 1 µM staurosporin (STS) [28] to induce apoptosis in presence of 50 µM zVAD-fmk to inhibit caspase activity and thus preserve cell morphology. After 6 to 8 hours, cells were fixed with formaldehyde 4% for 10 minutes and permeabilized with 0.5% Triton (5 minutes). After a 30 minutes incubation in a 0.2% gelatine – PBS 1x, cells were labelled with Anti-cytochrome c mouse mAb, (1/200, BD Biosciences) using 12-15 hours incubation at 4°C. After 3 rinses in PBS, cells were labeled Alexa Fluor 488 goat anti-mouse IgG (Molecular Probes) for one hour at room temperature. After a last rinse, the coverslips were mounted in 90% glycerine and imaged with successively confocal fluorescence and LISNA.

Acknowledgments

We thank Pierre Gonzales for COS7 cell cultures, Christelle Breillat and Delphine Bouchet-Teissier for neuron cultures, Paul Chabert and Pascal Berson for technical help. G.A. Blab acknowledges financial support by “Fonds zur Förderung der wissenschaftlichen Forschung” (FWF, Austria, Schrödinger-Stipendium) and the “Fondation pour la Recherche Médicale”

#85286 - $15.00 USD Received 17 Jul 2007; revised 7 Sep 2007; accepted 11 Sep 2007; published 12 Oct 2007

(FRM, France). This research was supported by CNRS (ACI Nanoscience and DRAB), Région Aquitaine, the French Ministry for Education and Research (MENRT), INSERM, Institut Bergonié, Ligue Contre Le Cancer and Association France Cancer.

#85286 - $15.00 USD Received 17 Jul 2007; revised 7 Sep 2007; accepted 11 Sep 2007; published 12 Oct 2007